Invariant NKT cells reduce the immunosuppressive activity of influenza A virus–induced myeloid-derived suppressor cells in mice and humans

Carmela De Santo,[1] Mariolina Salio,[1] S. Hajar Masri,[1] Laurel Yong-Hwa Lee,[1] Tao Dong,[1] Anneliese O. Speak,[2] Stefan Porubsky,[3] Sarah Booth,[1] Natacha Veerapen,[4] Gurdyal S. Besra,[4] Hermann-Josef Gröne,[3] Frances M. Platt,[2] Maria Zambon,[5] and Vincenzo Cerundolo[1]

[1]MRC Human Immunology Unit, Weatherall Institute of Molecular Medicine, John Radcliffe Hospital, Oxford, United Kingdom. [2]Department of Pharmacology, University of Oxford, Oxford, United Kingdom. [3]Division of Cellular and Molecular Pathology, German Cancer Research Center, Heidelberg, Germany. [4]School of Biosciences, University of Birmingham, Birmingham, United Kingdom. [5]Health Protection Agency, London, United Kingdom.

Infection with influenza A virus (IAV) presents a substantial threat to public health worldwide, with young, elderly, and immunodeficient individuals being particularly susceptible. Inflammatory responses play an important role in the fatal outcome of IAV infection, but the mechanism remains unclear. We demonstrate here that the absence of invariant NKT (iNKT) cells in mice during IAV infection resulted in the expansion of myeloid-derived suppressor cells (MDSCs), which suppressed IAV-specific immune responses through the expression of both arginase and NOS, resulting in high IAV titer and increased mortality. Adoptive transfer of iNKT cells abolished the suppressive activity of MDSCs, restored IAV-specific immune responses, reduced IAV titer, and increased survival rate. The crosstalk between iNKT and MDSCs was CD1d- and CD40-dependent. Furthermore, IAV infection and exposure to TLR agonists relieved the suppressive activity of MDSCs. Finally, we extended these results to humans by demonstrating the presence of myeloid cells with suppressive activity in the PBLs of individuals infected with IAV and showed that their suppressive activity is substantially reduced by iNKT cell activation. These findings identify what we believe to be a novel immunomodulatory role of iNKT cells, which we suggest could be harnessed to abolish the immunosuppressive activity of MDSCs during IAV infection.

Introduction

Influenza A virus (IAV) infection is a major public health threat, with significant morbidity and mortality in the young, elderly, and immunodeficient (1). There is evidence that pathological host responses, triggered by highly pathogenic IAV strains, including the pandemic 1918 H1N1 virus (2) and the more recent avian H5N1 virus (3), are critical to disease progression and dissemination. Although neutralizing Abs and T cell immunity control IAV clearance (4), the role played by cells of the innate arm of the immune system remains unclear.

Studies published over the last few years have shown that alteration of cytokines during polymicrobial sepsis (5), parasitic infections (6), vaccinia virus infection (7), and tumor development (8–11) causes a progressive accumulation of myeloid cells in the spleen, lymph nodes, and BM. These cells, which express CD11b and Gr-1 markers and have recently been named myeloid-derived suppressor cells (MDSCs) (12), comprise immature DCs (13), immature macrophages (14), and granulocytes (12). It has been shown that MDSCs are capable of suppressing T cell proliferation and promoting tumor growth (15), due to the expression of both NOS2 and arginase 1 (ARG1), resulting in the production of peroxynitrites under conditions of limited L-arginine availability (16). The use of selective inhibitors of NOS2 and ARG1 has confirmed the role of both enzymes in mediating MDSC suppressive activity (17, 18) and indicated that MDSCs can modulate antigen-specific immune responses during acute and chronic inflammatory conditions. Mechanisms that modulate the frequency and activity of MDSCs in vivo remain ill defined. However, it has been shown that CD1d-restricted NKT cells (type II NKT cells) can enhance MDSC suppressive activity by secreting IL-13 (19). It remains unclear whether invariant NKT cells (iNKT cells), which unlike type II NKT cells can be stained by CD1d/α-galactosylceramide (α-GalCer) tetramers, also play a role in modulating MDSC activity and phenotype.

iNKT cells are a subset of lymphocytes recognizing endogenous and/or exogenous glycolipid antigens in the context of CD1d molecules (20). Several articles have demonstrated that iNKT cells facilitate antimicrobial and antitumor responses by bridging the innate and adaptive immune systems (20). Mice lacking iNKT cells have an increased susceptibility to methylcholanthrene tumor induction, with earlier onset of the disease and a higher tumor incidence (21). Similarly, numerous studies have addressed the role of iNKT cells in bacterial (22, 23), mycotic (24), and parasitic infections (25, 26). Furthermore, mice deficient in CD1d-restricted T cells were shown to be more susceptible to infection with herpes simplex virus types 1 and 2 (HSV-1/HSV-2) (27, 28), cytomegalovirus (29), hepatitis B

Nonstandard abbreviations used: ARG1, arginase 1; B6, C57BL/6; α-GalCer, α-galactosylceramide; GSL, glycosphingolipid; HI, hemagglutination inhibition; IAV, influenza A virus; iGb3S, iGb3 synthase; iNKT cell, invariant NKT cell; MDSC, myeloid-derived suppressor cell; MLR, mixed lymphocyte reaction; PR8, Puerto Rico/8/34 IAV; TLR-L, TLR ligand.

Conflict of interest: The authors have declared that no conflict of interest exists.

Citation for this article: *J. Clin. Invest.* doi:10.1172/JCI36264.

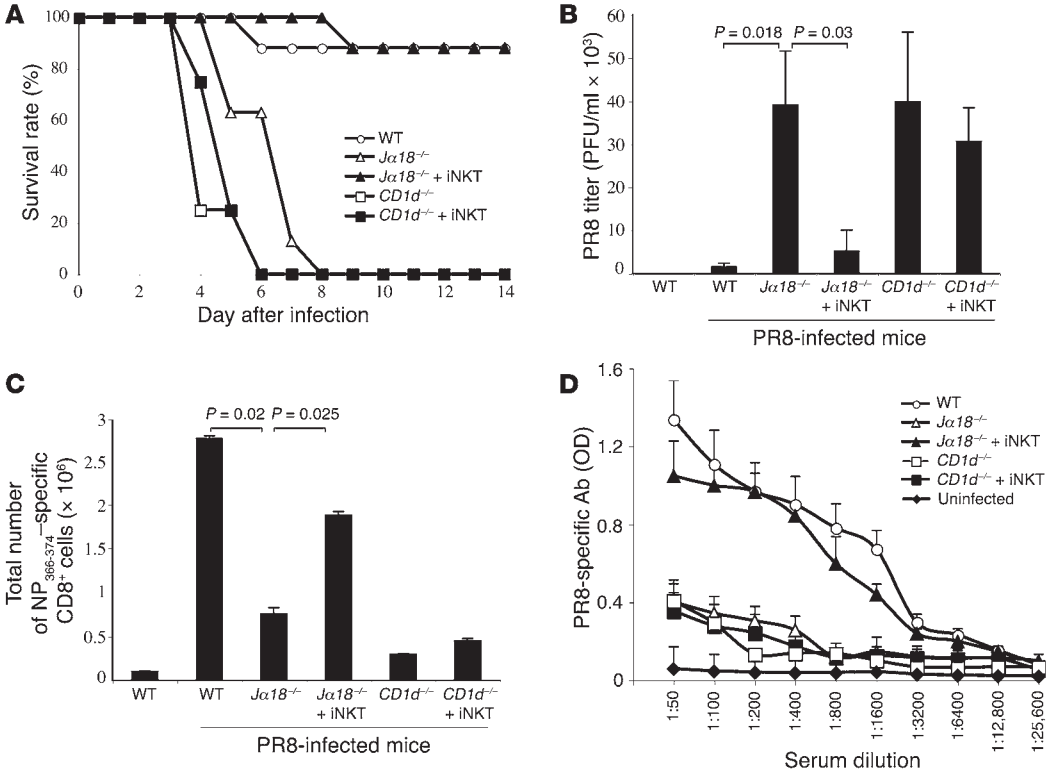

Figure 1
Adoptive transfer of iNKT cells mediates protection from lethal doses of PR8. WT, *Jα18*$^{-/-}$, and *CD1d*$^{-/-}$ mice (n = 8/group) were injected intranasally with PR8 (3 × 10^4 PFU/mouse). Liver-purified iNKT cells were adoptively transferred i.v. into *Jα18*$^{-/-}$ (*Jα18*$^{-/-}$ + iNKT) and *CD1d*$^{-/-}$ (*CD1d*$^{-/-}$ + iNKT) mice 1 day after infection. (**A**) Increased mortality of *Jα18*$^{-/-}$ mice following PR8 infection is prevented by the adoptive transfer of iNKT cells. Survival rate is shown as the percentage of live mice at different time points after the infection. Data are representative of 5 separate experiments. (**B**) PR8 titer in *Jα18*$^{-/-}$ mice is reduced by the adoptive transfer of iNKT cells. Lung homogenates from PR8-infected mice were assayed for number of PFU 6 days after infection. Results of statistical analyses, performed using Student's t test, are shown. (**C**) Total number of $NP_{366–374}$–specific CTLs in PR8-infected *Jα18*$^{-/-}$ mice is restored by the adoptive transfer of iNKT cells. The number of $NP_{366–374}$–specific CTLs represents the average (±SD) of results obtained in n = 8 mice/group. Results of statistical analyses, performed using Student's t test, are shown. (**D**) Anti-PR8 Ab titers in PR8-infected *Jα18*$^{-/-}$ mice are restored by the adoptive transfer of iNKT cells. The titer of anti-PR8–specific IgG was measured 6 days after infection.

virus replication (30), and diabetogenic encephalomyocarditis virus (31). In CD1d-deficient BALB/c mice, numbers of respiratory syncytial virus–specific (RSV-specific) CD8$^+$ MHC class I–restricted T cells were reduced, suggesting that CD1d-restricted T cells influence the adaptive immune response to RSV infection (32). The activity of iNKT cells against viral infections is further confirmed by the presence of viral mechanisms capable of downregulating CD1d molecules (33–35). However, it remains unclear whether iNKT cells can facilitate IAV-specific immune responses, contributing to survival of IAV-infected mice. Although recent results have indicated that iNKT cell activation improves disease course in IAV infection (36), it has previously been shown that priming of *CD1d*$^{-/-}$ mice with small doses of IAV enhanced their survival rate after challenge with lethal doses of IAV (37). These results are consistent with the possibility that CD1d-restricted cells, including iNKT cells, are not necessary for protection against IAV. Alternatively, priming of *CD1d*$^{-/-}$ mice with small doses of IAV may induce protective IAV-specific immune responses capable of protecting *CD1d*$^{-/-}$ mice from a subsequent challenge with higher IAV doses. No experiments were carried out to distinguish between these two possibilities, and to date no articles to our knowledge have described the survival rate of naive *CD1d*$^{-/-}$ or *Jα18*$^{-/-}$ (i.e., iNKT$^{-/-}$) mice injected with lethal doses of IAV. Although there is evidence that iNKT cells play an important role in combating viral infections, the mechanisms by which iNKT cells control viral infections remain unclear.

In this article, we have analyzed the crosstalk between iNKT cells and MDSCs and demonstrated that iNKT cells are able to control the frequency and activity of MDSCs during IAV infection, preventing IAV-induced high mortality rate and ensuring optimal IAV-specific immune response. These results underscore what we believe to be a previously unknown role of iNKT cells in abolishing MDSC suppressive activity and indicate that harnessing iNKT cells in vivo could assist antigen-specific immune responses by enhancing DC maturation and B cell activation, while minimizing MDSC suppressive activity.

Results

iNKT cell–dependent resistance to lethal intranasal injection of the IAV A/Puerto Rico/8/34. To assess whether iNKT cells play a role in controlling IAV infection, iNKT-deficient and *CD1d*$^{-/-}$ mice were infected with IAV A/Puerto Rico/8/34 (PR8) (38). We observed that

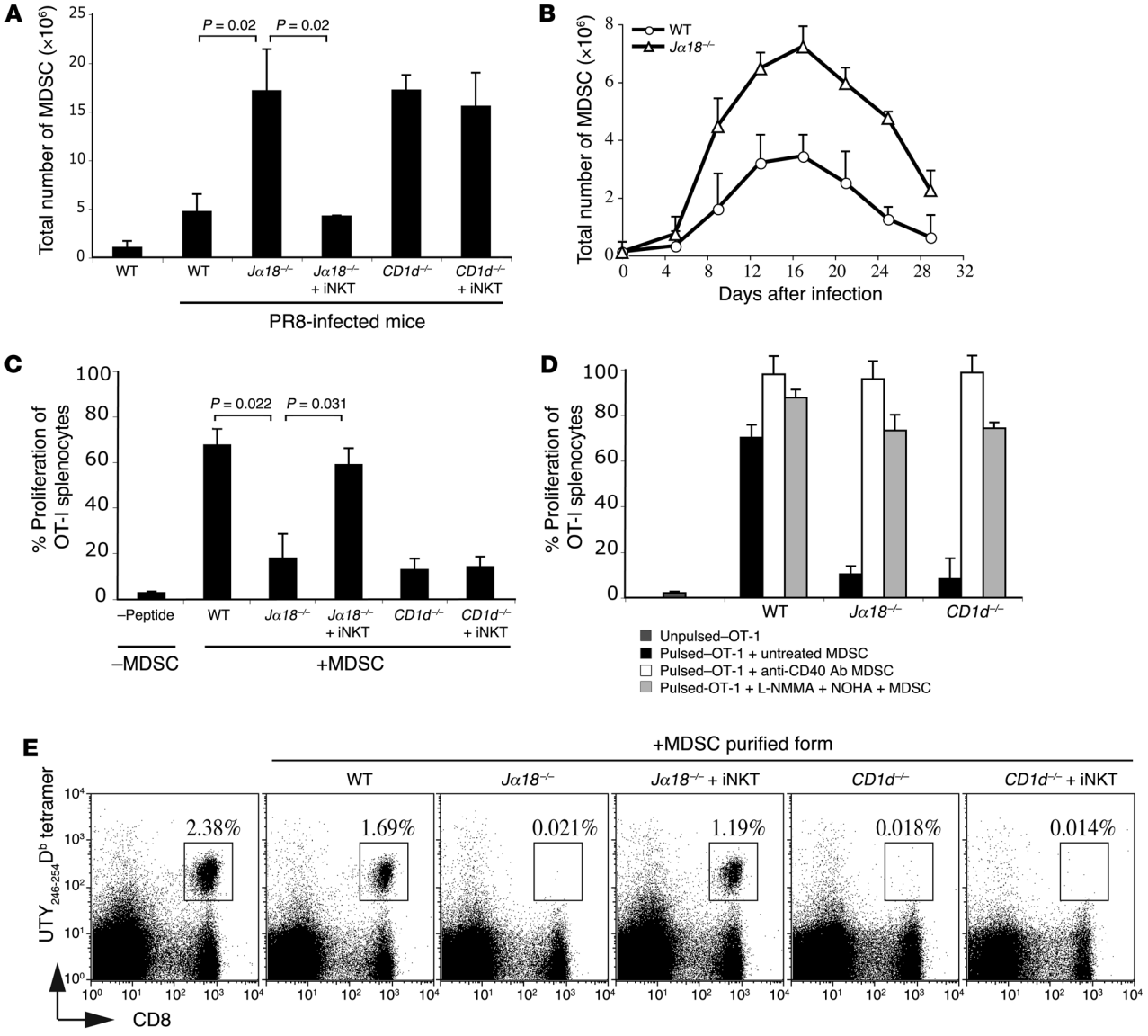

Figure 2

Adoptive transfer of iNKT cells reduces PR8-induced MDSC expansion. (**A**) iNKT cells adoptively transferred into PR8-infected *Jα18*$^{-/-}$ mice reduced the total number of lung MDSCs. PR8-infected WT, *Jα18*$^{-/-}$, and *CD1d*$^{-/-}$ mice were injected with iNKT cells. Lung homogenates were stained with CD11b and Gr-1 Abs. (**B**) Injection of sublethal doses of PR8 (3×10^2 PFU) reduces the total numbers of lung MDSCs. (**C**) Adoptive transfer of iNKT cells reduces in vitro suppressive activity of PR8-induced MDSCs. MDSCs were purified from lungs of PR8-infected mice and cocultured with CFSE-labeled OT-I splenocytes. (**D**) The suppressive activity of MDSCs from PR8-infected mice is reduced by treatment with anti–CD40 agonist Ab and NOS2 and ARG1 inhibitors. Lung-purified MDSCs were left untreated (black bars) or treated in vitro with either anti–CD40 agonist Ab (white bars) or with N^G-monomethyl-L-arginine (L-NMMA) and NOHA (light gray bars) and then added to OT-I splenocytes. Proliferation of unpulsed OT-I splenocytes in the absence of MDSCs is shown (dark gray bars). (**E**) Adoptive transfer of MDSCs from infected mice suppresses the expansion of $UTY_{246–254}$–specific $CD8^+$ T cell responses. $UTY_{246–254}$ CTL responses were assessed in vaccinated mice injected with MDSCs from PR8-infected mice (see Methods). H-$2D^b$/$UTY_{246–254}$ tetramer ($UTY_{246–254}D^b$ tetramer) versus CD8 dot plots are shown for gated propidium iodide–negative lymphocytes, and the percentage of cells staining positively with the tetramers is indicated. In **A**–**E**, data represent the average ± SD of $n = 5$ mice/group, and results of statistical analyses, performed using Student's *t* test, are shown.

injection of high doses of PR8 (3×10^4 PFU) into *Jα18*$^{-/-}$ and *CD1d*$^{-/-}$ mice resulted in increased mortality, as compared with the mortality rate of PR8-infected WT mice (Figure 1A). Consistent with these results, PR8-infected *Jα18*$^{-/-}$ and *CD1d*$^{-/-}$ mice had higher IAV titer (Figure 1B) and reduced percentage and absolute numbers of both PR8-specific $CD8^+$ T lymphocytes (Figure 1C and data not shown) and Abs (Figure 1D), when compared with PR8-infected WT mice. Since iNKT cell frequency was enhanced in the lungs of PR8-infected WT mice (data not shown), we assessed whether adoptive transfer of iNKT cells into PR8-infected *Jα18*$^{-/-}$ mice could enhance survival rate. We observed that the adoptive transfer of iNKT cells into PR8-infected *Jα18*$^{-/-}$ mice rescued the survival of a large proportion

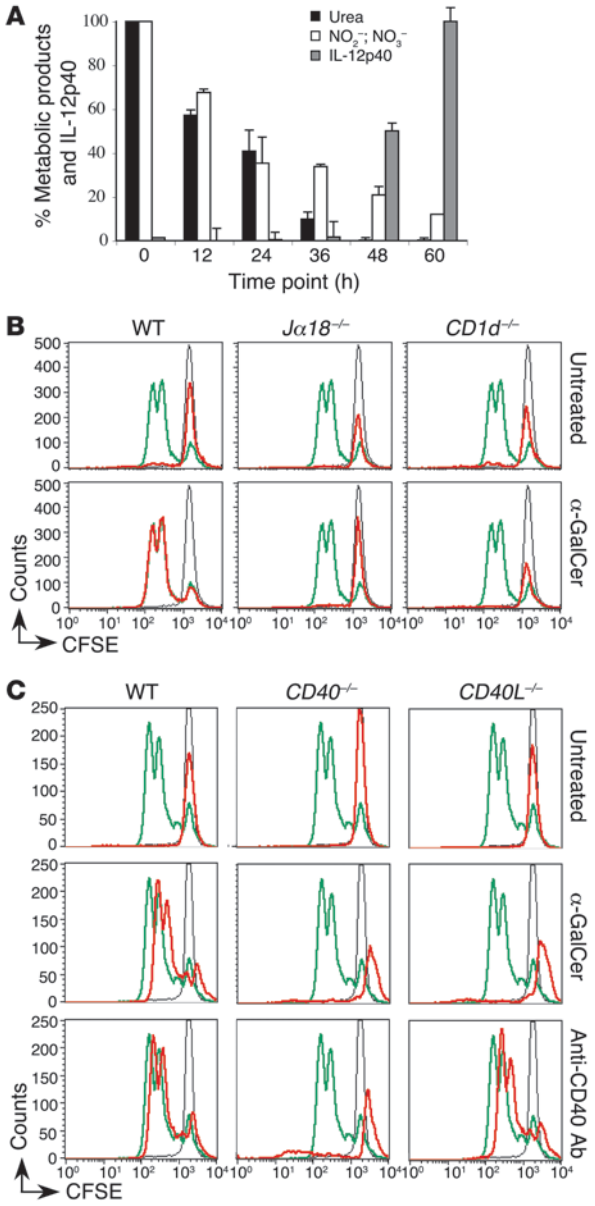

Figure 3
The crosstalk between iNKT and MDSCs is CD1d and CD40 dependent. (**A**) Loss of ARG1 and NOS2 activity in α-GalCer–pulsed MDSCs incubated with BM-derived iNKT cells. MDSCs were treated with α-GalCer in the presence of iNKT cells and collected at different time points. ARG1 and NOS2 activities were measured using a colorimetric assay to evaluate urea and nitrate/nitrite release, respectively (17, 18). An ELISA was used to evaluate IL-12p40 production. Values are shown as a percentage relative to time point 0. The maximum amount of urea released by untreated MDSCs (1×10^6) was 91.7 μg. The maximum amount of NO_2^- and NO_3^- measured in the supernatant of untreated MDSCs was 120 μM. The maximum amount of IL-12p40 was 200 ng/ml. (**B**) Incubating α-GalCer–pulsed MDSCs with BM-derived iNKT cells abolishes their suppressive function. CFSE-labeled OT-I cell proliferation was analyzed in the presence (red) or absence (green) of MDSCs derived from WT, *Jα18*$^{-/-}$, or *CD1d*$^{-/-}$ mice. MDSCs were left untreated or pulsed with α-GalCer. Proliferation of OT-I cells without SIINFEKL peptide is superimposed in all panels (black). (**C**) The effect of iNKT cells on α-GalCer–pulsed MDSCs is CD40 dependent. CFSE-labeled OT-I proliferation was analyzed in the presence (red) or absence (green) of MDSCs derived from WT, *CD40*$^{-/-}$, or *CD40L*$^{-/-}$ mice. MDSCs were left untreated or pulsed with α-GalCer. To assess the role of the CD40 molecules, BM-derived MDSCs were treated with anti–CD40 agonist Ab for 48 hours. Proliferation of CFSE-labeled OT-I cells without SIINFEKL peptide is superimposed in all panels (black).

of infected mice (Figure 1A) and was associated with an increase in the frequency and absolute numbers of PR8-specific T cell and Ab responses (Figure 1, C and D, and data not shown) and with a reduction of IAV titer (Figure 1B). We confirmed that the protective effect of the adoptively transferred liver purified iNKT cells into PR8-infected *Jα18*$^{-/-}$ mice was iNKT cell dependent by demonstrating that injection of liver-purified lymphocytes, sorted with anti–TCR-β and -CD5 and depleted of iNKT cells by CD1d/α-GalCer tetramer–guided sorting, failed to increase the survival of PR8-infected *Jα18*$^{-/-}$ mice (Supplemental Figure 1; supplemental material available online with this article; doi:10.1172/JCI36264DS1). Furthermore, to rule out that the protective effect of the adoptively transferred iNKT cells was due to their in vitro activation by the anti–TCR-β Ab, we demonstrated that the injection of iNKT cells into PR8-infected *CD1d*$^{-/-}$ mice failed to protect them from PR8 infection and did not have any effect on PR8 virus titer and PR8-specific immune responses (Figure 1).

These results indicate that iNKT cells play an important role in controlling IAV PR8 virus infection and that this effect is CD1d dependent.

Adoptive transfer of iNKT cells significantly reduces the suppressive activity of PR8-expanded MDSCs. It has previously been shown that lungs of IAV-infected mice are infiltrated by neutrophils expressing CD11b and Gr-1 markers (39, 40). Since it is known that alteration of cytokines during acute and chronic inflammations results in the expansion of ARG-1– and NOS-expressing MDSCs (i.e., $CD11b^+Gr\text{-}1^+$ cells) (10) and since cytokines and chemokines are elevated during influenza virus infection (3, 41), we measured the frequency and activity of MDSCs in the lungs of PR8-infected WT, *Jα18*$^{-/-}$, and *CD1d*$^{-/-}$ mice (Figure 2A). We observed an expansion of the percentage and absolute numbers of MDSCs in PR8-infected mice, which was greater in infected *Jα18*$^{-/-}$ and *CD1d*$^{-/-}$ mice than in infected WT mice (Figure 2A and data not shown). It is worth noting that infection of WT mice with PR8 induces an expansion of MDSCs (~5%), as compared with the percentage of MDSCs present in naive WT mice (Figure 2A). Importantly, injection of iNKT cells in *Jα18*$^{-/-}$ mice, but not in *CD1d*$^{-/-}$ mice, resulted in the reduction of MDSCs (Figure 2A). A large proportion of PR8-induced MDSCs in WT and *Jα18*$^{-/-}$ mice expressed CD1d, CD40, and the neutrophil marker 7/4 (data not shown). Injection of lower doses of PR8 (3×10^2 PFU), while confirming the higher frequency of MDSCs in *Jα18*$^{-/-}$ than in WT mice, showed that *Jα18*$^{-/-}$ mice were capable of controlling sublethal PR8 infection and that the numbers of PR8-induced MDSCs declined to background levels by day 30 after the infection (Figure 2B).

To investigate the functional activity of PR8-induced MDSCs, we set up a proliferation assay using CFSE-labeled OT-I cells as responders. Consistent with the observation that PR8 infection of WT mice induces a small but reproducible increase in MDSCs (Figure 2A), we demonstrated that MDSCs purified from PR8-infected WT mice induced a partial inhibition of OT-I proliferation (~25%–30% inhibition). However, MDSCs isolated from the lungs of PR8-infected *Jα18*$^{-/-}$ and *CD1d*$^{-/-}$ mice, when normalized

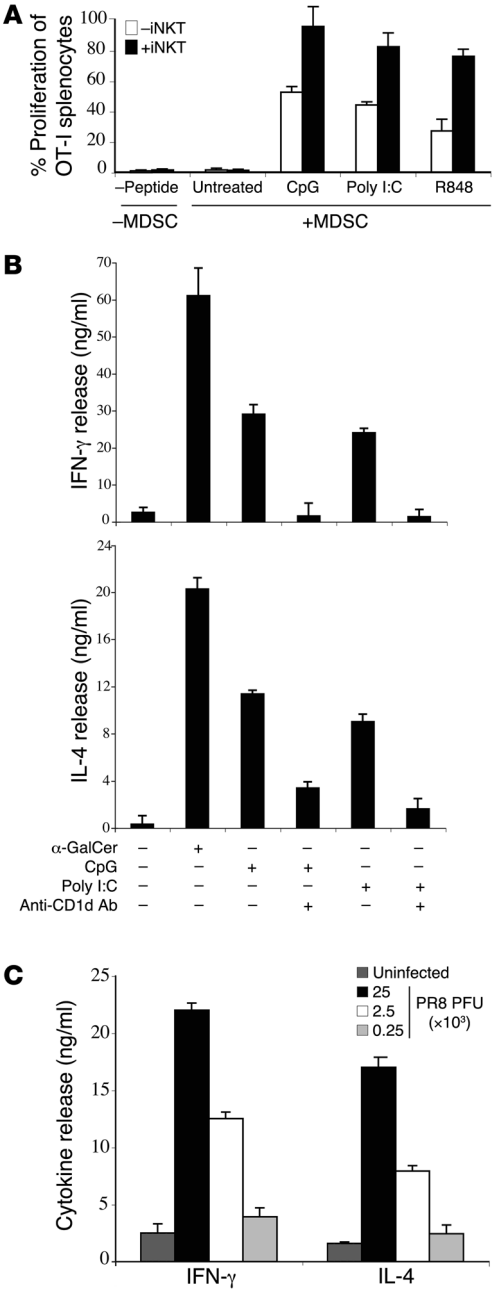

Figure 4
Infection of MDSCs with PR8 fosters their ability to activate iNKT cells. (**A**) TLR agonists rescue suppressive activity of MDSCs. BM-derived MDSCs were treated with TLR agonists in the presence or absence of liver-purified iNKT cells as described in Methods. CFSE-labeled OT-I proliferation was analyzed after addition of TLR agonist–treated MDSCs in the presence (black bars) or absence (white bars) of iNKT cells. Data represent the average ± SD of 3 replicates and are representative of 3 separate experiments. As negative control, proliferation of unpulsed CFSE-labeled OT-I splenocytes in the absence of MDSCs is shown. (**B**) IFN-γ and IL-4 release from iNKT cells incubated for 48 hours with CpG- or poly I:C–treated MDSCs, in the presence or absence of anti-CD1d blocking Ab. Data represent the average ± SD of 3 replicates and are representative of 3 separate experiments. (**C**) Amounts of IFN-γ and IL-4 released by iNKT cells incubated in the presence of MDSCs infected with increasing doses of PR8.

for the same number of cells added to OT-I splenocytes, showed a significantly greater suppressive activity on in vitro proliferation of CFSE-labeled OT-I splenocytes (Figure 2C). In addition, their adoptive transfer into naive mice inhibited the ability of recipients to mount antigen-specific immune responses (Figure 2E). To identify the mechanisms controlling PR8-induced MDSC–mediated suppressive activity, we established that OT-I proliferation could be rescued either by treatment of MDSCs with inhibitors of ARG1 and NOS activity or by incubating them with anti–CD40 agonist Ab (Figure 2D). Finally, adoptive transfer of iNKT cells into *Jα18*$^{-/-}$ mice significantly reduced both in vitro and in vivo the suppressive activity of PR8-induced MDSCs to levels similar to those observed with MDSCs purified from PR8-infected WT mice, while adoptive transfer of iNKT cells into *CD1d*$^{-/-}$ mice had no effect on the suppressive activity of PR8-induced MDSCs (Figure 2, C and E).

These results demonstrate that lungs of *Jα18*$^{-/-}$ and *CD1d*$^{-/-}$ mice infected with PR8 have higher numbers of infiltrating MDSCs compared with WT mice and identify the suppressive mechanisms by which lung-infiltrating MDSCs inhibit T cell proliferation, highlighting a direct link between the presence of iNKT cells in PR8-infected mice and lack of suppression by MDSCs.

The ability of iNKT cells to reduce the suppressive activity of MDSCs is CD40-CD40L dependent. In order to further study the crosstalk between iNKT cells and MDSCs and understand the mechanisms by which iNKT cells abolish PR8-induced suppressive activity of MDSCs, further experiments were carried out using BM-derived MDSCs. We confirmed that GM-CSF–differentiated BM-derived MDSCs express CD11b, Gr-1, CD1d, and CD40 (Supplemental Figure 2A) and have ARG1 and NOS2 activity, as defined by their ability to generate urea and peroxynitrites (Figure 3A, time point 0 hours) (42). We also demonstrated that BM-derived MDSCs were capable of inhibiting in vitro proliferation of splenocytes from OT-I mice (Figure 3B, top left panel), even in the presence of peptide-pulsed matured DCs (Supplemental Figure 2B). Pulsing MDSCs with 100 ng of the iNKT cell agonist α-GalCer in the presence of iNKT cells (Supplemental Figure 2C) led to the reduction of ARG1 and NOS2 activity and to the enhanced secretion of IL-12p40 (Figure 3A). No secretion of IL-23 and IL-12p70 was observed (data not shown). Although previous reports have demonstrated that IL-12p40 reduces IL-12–mediated Th1 responses in vivo by blocking the binding of IL-12 or IL-23 to their receptors (43, 44), it is unlikely that the enhanced secretion of IL-12p40 by MDSCs either treated with TLR ligands (TLR-Ls) (see below) or incubated with iNKT cells had an inhibitory effect, as defined by the in vivo and in vitro enhanced immune responses. As a control, we confirmed that MDSCs pulsed with 100 ng of α-GalCer were not lysed by iNKT cells (Supplemental Figure 3) and that incubation of CFSE-labeled α-GalCer–pulsed CD11c^{-} MDSCs with iNKT cells led to their differentiation into CD11c^{+} cells (Supplemental Figure 3) and upregulation of CD86 and MHC class II expression (data not shown).

We further investigated the effect of α-GalCer on BM-derived MDSC suppressive activity by assessing their ability to suppress CFSE-labeled OT-I proliferation (Figure 3, B and C). We showed that pulsing MDSCs with α-GalCer in the presence of BM-resident iNKT cells from WT mice (Supplemental Figure 2C) completely relieved MDSC suppression (Figure 3B, bottom left), as compared

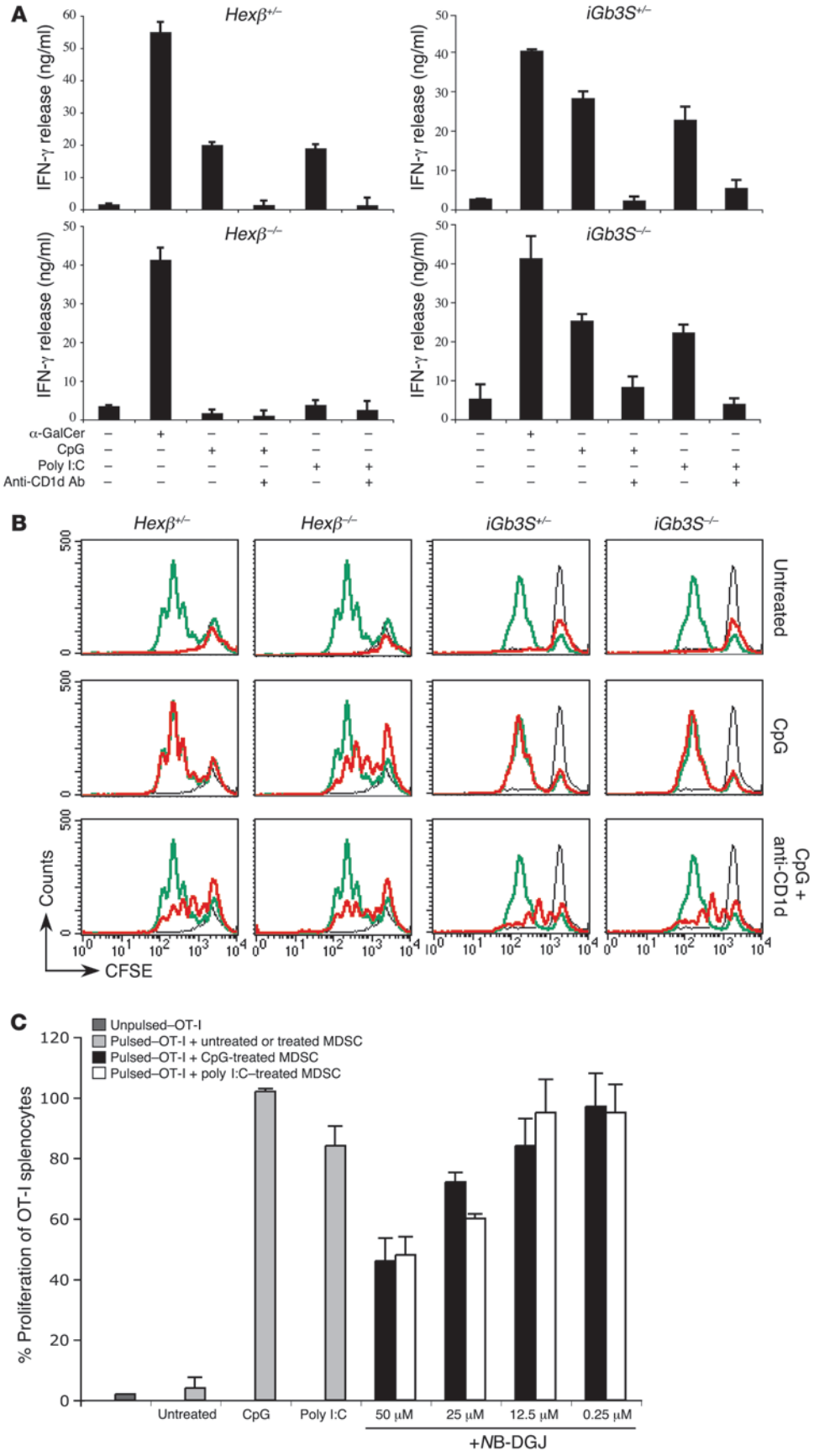

Figure 5

TLR-L–treated MDSCs derived from *Hexβ*$^{-/-}$ mice fail to stimulate iNKT cells. (**A**) iNKT cells derived from WT mice fail to produce IFN-γ when incubated with TLR-L–matured MDSCs derived from *Hexβ*$^{-/-}$ mice. IFN-γ secretion by iNKT cells derived from WT mice, coincubated with TLR-L–matured MDSCs derived from *Hexβ*$^{-/-}$ or *iGb3S*$^{-/-}$ mice. Different protocols are indicated. (**B**) CpG-treated *Hexβ*$^{-/-}$ MDSCs fail to foster the crosstalk between iNKT cells and MDSCs. CFSE-labeled OT-I proliferation in the presence of TLR-L–treated MDSCs derived from either *Hexβ*$^{-/-}$ or *iGb3S*$^{-/-}$ mice is shown. BM-derived *Hexβ*$^{-/-}$ and *iGb3S*$^{-/-}$ MDSCs were treated with CpG in the presence or absence of blocking anti-CD1d Ab. Proliferation of OT-I cells in the presence (red) or absence (green) of MDSCs is shown. Proliferation without the SIINFEKL peptide (black) is superimposed in all panels. (**C**) Inhibition of GSL biosynthesis in TLR-L–matured MDSCs reduces iNKT cell activation. MDSCs derived from WT mice were incubated with either poly I:C or CpG and then treated with increasing concentrations of *N*-butyldeoxygalactonojirimycin (*N*B-DGJ). MDSCs were incubated with iNKT cells for 24 hours and tested for their effect on OT-I proliferation (see Methods). Addition of *N*B-DGJ to OT-I splenocytes in the absence of MDSCs did not affect OT-I proliferation (data not shown). Proliferation of unpulsed OT-I splenocytes in the absence of MDSCs is shown (dark gray). Treatment of MDSCs with TLR-L (light gray bars) relieves CFSE-labeled OT-I proliferation, as compared with the lack of OT-I proliferation observed after addition of untreated MDSCs. In contrast, combined treatment of MDSCs with either CpG (black bars) or poly I:C (white bars) plus increasing doses of *N*B-DGJ reduces OT-I proliferation.

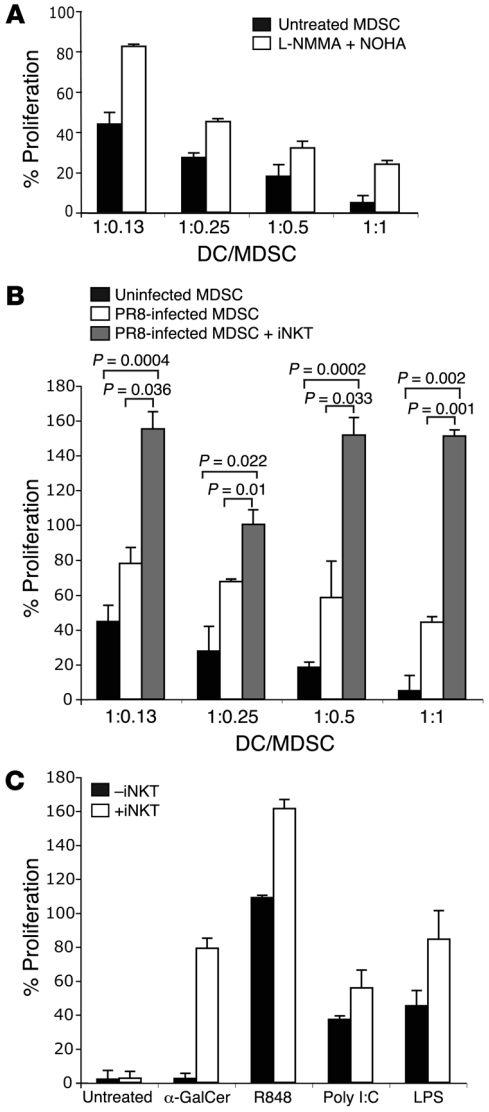

Figure 6
Inhibition of alloreactive T cell proliferation by human MDSCs can be rescued by iNKT cells. (**A**) Healthy donors' GM-CSF–differentiated MDSCs have MLR-suppressive activity, which can be blocked by the addition of NOHA and L-NMMA. The data are expressed as described in Methods. Addition of NOHA and L-NMMA to the MLR in the absence of MDSCs does not affect PBL proliferation (data not shown). The ratio of DCs to human GM-CSF–treated MDSCs is shown. (**B**) PR8 infection of healthy donors' GM-CSF–treated MDSCs rescues MLR proliferation. Human GM-CSF–treated MDSCs were left untreated (black bars) or infected with PR8 and cocultured in the presence (gray bars) or absence (white bars) of iNKT cells (2.5×10^4) for 24 hours. After irradiation, PR8-infected and uninfected MDSCs were added to the MLR. The data are expressed as described in Methods. The ratio of DCs to human MDSCs used is shown. Results of statistical analyses, performed using Student's *t* test, are shown. (**C**) TLR-L incubation of healthy donors' GM-CSF–differentiated MDSCs rescues T cell proliferation. Human GM-CSF–treated MDSCs were treated with LPS (10 μg/ml), R848 (5 μg/ml), poly I:C (10 μg/ml), or α-GalCer (100 ng/ml) and cocultured in the presence (white bars) or absence (black bars) of iNKT cells for 24 hours. The data are expressed as described in Methods. The ratio of DCs to human GM-CSF–treated MDSCs used was 1:1.

with BM-derived cells from *Jα18*$^{-/-}$ (Figure 3B, top and bottom middle panels) and *CD1d*$^{-/-}$ mice (Figure 3B, top and bottom right panels). The effect of iNKT cells on MDSC suppressive activity was CD40 and CD40L dependent, as defined by the results of experiments carried out with *CD40*$^{-/-}$ and *CD40L*$^{-/-}$ mice (Figure 3C, middle row, middle and right panels) and the use of agonist anti-CD40 Ab (Figure 3C, bottom row, middle and right panels).

Collectively, our findings demonstrate that the in vitro activation of iNKT cells by α-GalCer–pulsed MDSCs leads to phenotypic and functional differentiation of MDSCs, events that are dependent on CD40-CD40L interaction.

TLR-L treatment and IAV infection of MDSCs relieves MDSC suppressive activity. Since it has previously been shown that TLR-dependent maturation of DCs can foster the interaction between DCs and iNKT cells (20, 45–47), we assessed whether either incubation of MDSCs with TLR-L or infection of MDSCs with IAV, in the presence or absence of iNKT cells, could modulate MDSC suppressive activity. We showed that incubation of MDSCs with TLR3 (poly I:C), TLR7/8 (R848), and TLR9 (CpG 2216) agonists, in the absence of iNKT cells, partially relieved MDSC suppressive activity on CFSE-labeled OT-I proliferation (Figure 4A) and resulted in IL-12p40 secretion (data not shown). We showed that addition of iNKT cells to TLR-L–treated MDSCs further reduced MDSCs dependent suppressive activity (Figure 4A) and enhanced IL-12p40 production (data not shown). It is worth noting that LPS failed to relieve MDSC suppressive activity, at a broad range of different concentrations, in both the presence and absence of iNKT cells (data not shown). Subsequent experiments demonstrated that CpG and poly I:C–treated MDSCs were capable of activating iNKT cells and that such activation was CD1d dependent, as defined by the lack of IFN-γ and IL-4 secretion in the presence of anti CD1d-blocking Abs (Figure 4B).

The capacity of a range of TLR-Ls to reduce MDSC-dependent suppressive activity raised the possibility that the ability of iNKT cells to reduce the MDSC suppressive activity in PR8-infected mice could be accounted for by direct crosstalk between PR8-infected MDSCs and iNKT cells. Consistent with the observation that lung-infiltrating MDSCs purified from PR8-infected mice are infected by PR8 virus (Supplemental Figure 4A), we showed that BM-derived MDSCs could be infected by PR8 (Supplemental Figure 4B) and that PR8-infected MDSCs were capable of activating iNKT cells, as defined by the secretion of IFN-γ and IL-4 (Figure 4C).

These results are consistent with the observation that TLR-L–treated MDSCs can foster the interaction with iNKT cells and provide important insights into the mechanisms controlling the crosstalk between iNKT cells and MDSCs in PR8-infected mice.

MDSCs derived from a mouse model of glycosphingolipid storage disease fail to stimulate iNKT cells. To further investigate the mechanisms that control the crosstalk between iNKT cells and TLR-L–treated MDSCs, we used MDSCs derived from β-hexosaminidase A/B–deficient (*Hex*β$^{-/-}$) mice, which are unable to activate iNKT cells due to the accumulation of glycosphingolipids (GSLs) in the endolysosomal compartment (48–50). We showed that the crosstalk between iNKT cells and CpG- or poly I:C–treated MDSCs is compromised in GSL storage disorders (Figure 5, A and B), although TLR-L incubation of *Hex*β$^{-/-}$ derived MDSCs upregulates CD1d expression and results in enhanced IL-12 secretion (Supplemental Figure 5). The partial proliferation of OT-I splenocytes in the

Table 1
IAV-specific Ab titer from collected blood samples

Donors	Date of blood collection	Anti-H3N2 Ab titer		Anti-H1N1 Ab titer	
		A/Wisconsin/67/2005	A/Wellington/1/2004	A/Solomon Islands/03/2006	A/New Caledonia/20/92
Donor 1	August 4, 2006	<10	<10	<10	<10
	May 1, 2007	<10	64	<10	<10
Donor 2	October 24, 2006	<10	<10	<10	<10
	April 24, 2007	64	128	<10	<10
Donor 3	October 6, 2006	<10	16	<10	<10
	January 25, 2007	32	64	<10	<10
Donor 4	December 9, 2005	<10	<10	<10	<10
	July 21, 2006	<10	<10	<10	<10
Donor 5	March 15, 2006	<10	<10	<10	<10
	October 13, 2007	<10	<10	<10	<10
Donor 6	April 10, 2006	64	128	<10	<10
Donor 7	January 11, 2007	<10	<10	256	128
Donor 8	November 6, 2007	<10	<10	128	128
Donor 9	January 5, 2006	<10	<10	64	256
Donor 10	August 10, 2006	<10	16	<10	<10

HI assay using indicated strains of IAV. Blood samples from donors 1, 2, and 3 were collected either before (first time point) or within 30–60 days (second time point) after onset of acute respiratory illness. Blood samples from donors 4 and 5 were collected at the indicated time points in the absence of any acute respiratory illness. Blood samples from donors 6, 7, 8, 9, and 10 were collected shortly after (between 15 and 30 days) onset of acute respiratory illness. Values shown as <10 indicate undetectable Ab titers.

presence of *Hex*β$^{-/-}$ derived MDSCs treated with CpG (Figure 5B) is due to a direct effect of TLR9 signaling events on MDSCs, which is consistent with the results shown in Figure 4A, indicating that incubation of MDSCs with the TLR9 agonist CpG, in the absence of crosstalk with iNKT cells, results in a partial relief of MDSC suppressive activity on OT-I proliferation. We extended these results by demonstrating that incubation of CpG- and poly I:C–treated MDSCs with the specific inhibitor of GSL biosynthesis *N*-butyldeoxygalactonojirimycin (*N*B-DGJ) (51) reduced the ability of iNKT cells to relieve the suppressive activity of MDSCs, as defined by reduced CFSE-labeled OT-I proliferation (Figure 5C). Consistent with previous findings (45, 46), these results indicate that TLR agonists, in addition to having a direct maturation effect on MDSCs, induce the upregulation of endogenous iNKT cell ligand(s), which results in the activation of iNKT cells and further relief of MDSC suppressive activity. Incubation of *Hex*β$^{-/-}$ derived cells with TLR-L, while failing to facilitate the crosstalk between MDSCs and iNKT cells, does not abolish a direct TLR-L maturation effect on MDSCs, which results in partial relief of MDSC suppressive activity.

Based on investigations in *Hex*β$^{-/-}$ mice, iGb3 was proposed to be the endogenous ligand essential for the positive selection of mouse iNKT cells in the thymus (48). Although iGb3 can stimulate iNKT cells in vitro (48, 52), there is currently no direct evidence supporting the hypothesis that iGb3 plays a role as an endogenous selecting ligand in vivo. Furthermore, studies in iGb3 synthase–deficient (*iGb3S*$^{-/-}$) mice, with a deletion of the catalytic region of the *iGb3S* gene, demonstrated that in the absence of detectable isoglobo-series of GSLs (iGb3, iGb4, and iGb5), the frequency and phenotype of iNKT cells were not altered (53). We have now extended these results by demonstrating that iGb3 is not necessary for the crosstalk between iNKT cells and CpG-matured MDSCs, since CpG-treated MDSCs derived from *iGb3S*$^{-/-}$ mice were still able to activate in a CD1d-dependent manner liver-purified iNKT cells from WT mice (Figure 5, A and B, right panels, and Supplemental Figure 5A).

These results indicate that the crosstalk between iNKT cells and TLR-L–matured MDSCs is prevented by conditions in which loading of endogenous ligand(s) onto CD1d molecules is compromised either by the accumulation of GSL endolysosomal storage or by alteration of GSL biosynthesis.

Expansion of human MDSCs during IAV infection. Having characterized the interaction between mouse iNKT cells and MDSCs derived from an IAV infection model, we extended these results by assessing whether human iNKT cells have a similar effect on human MDSCs. We showed that incubation of healthy donor CD11b$^+$ monocytes with low doses of GM-CSF (5 ng/ml) led to their differentiation into cells capable of suppressing T cell proliferation in a mixed lymphocyte reaction (MLR) (Figure 6A). Consistent with recently published data (54), a similar inhibition of T cell proliferation was obtained by sorting CD14$^+$ cells and incubating them with GM-CSF (data not shown). The suppressive activity of GM-CSF–differentiated CD11b$^+$ cells could be pharmacologically relieved by adding inhibitors of ARG1 and NOS2 (Figure 6A). Interestingly, we showed that the suppressive activity of GM-CSF–treated CD11b$^+$ cells was relieved by either PR8 infection (Figure 6B) or incubation with TLR-L in the presence of added human iNKT cells (Figure 6C). These results are consistent with our previous findings obtained with mouse MDSCs and demonstrate that incubation of human GM-CSF–differentiated CD11b$^+$ cells with either IAV or TLR-L enhances their ability to crosstalk with human iNKT cells, thus restoring optimal MLR proliferation.

It has previously been shown that MDSCs are expanded in tumor patients (9). However, it remains unclear whether immunosuppressive monocytes are expanded during viral infections in humans and whether harnessing iNKT cells can abolish their suppressive activity. To address these questions, we collected CD11b$^+$ cells from PBLs of individuals at 2 different time points: while they were clinically healthy (first time point) and within 30–60 days after respiratory illness onset (second time point) (Figure 7 and Table 1). To prove that the respiratory illness was caused by IAV infection, ex vivo analysis of the suppressive activity of CD11b$^+$ cells was correlated with the hemagglutination inhibition (HI) Ab titer specific for H3N2 and H1N1 IAV strains, which circulated during the time period over which the human material was collected (Table 1).

The results of these experiments showed that ex vivo purified peripheral blood CD11b$^+$ cells collected at the time of IAV seroconversion suppressed MLR proliferation (Figure 7, A–C), as compared with MLR proliferation obtained with CD11b$^+$ cells purified from the same individuals before the respiratory symptoms and

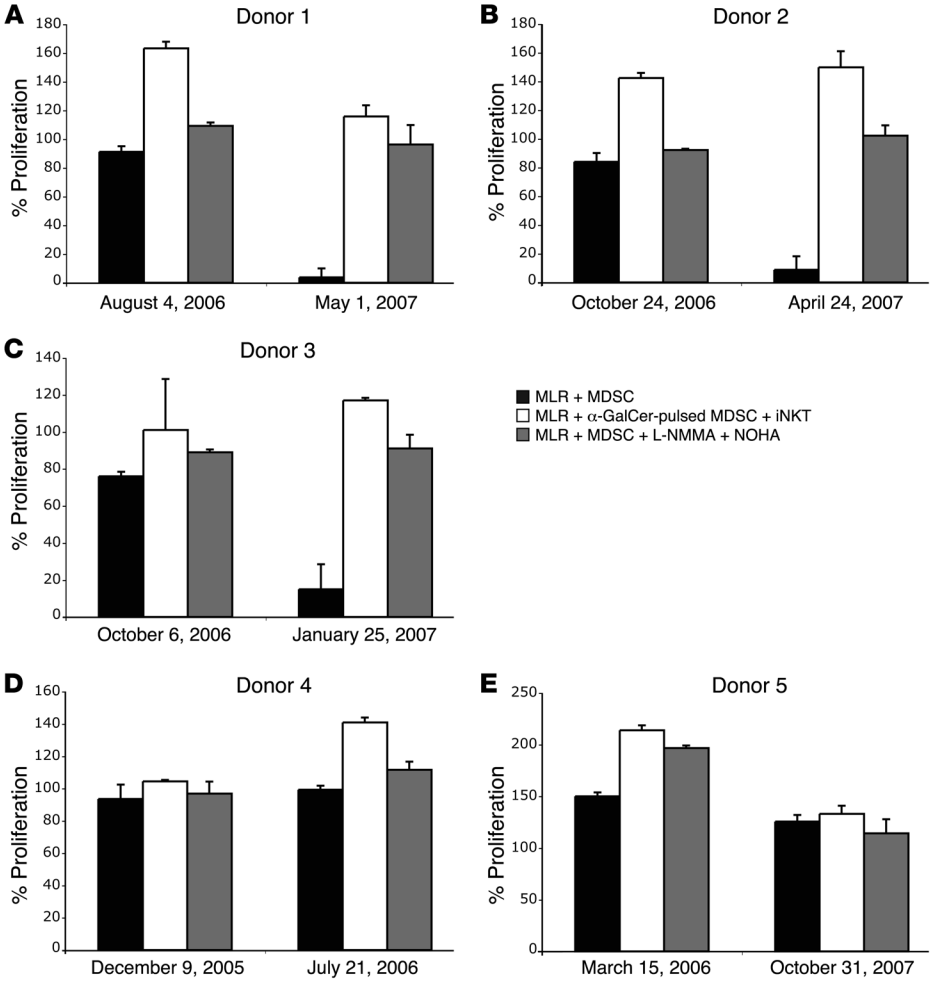

Figure 7
Inhibition of T cell proliferation by MDSCs purified from IAV-infected individuals. CD11b$^+$ cells were bead purified from PBLs derived from either IAV-infected individuals (**A**–**C**) or healthy donors (**D** and **E**). All donors were bled twice. For donors 1, 2, and 3, the first blood sample was collected before the clinical symptom onset, while the second blood sample was collected within 30–60 days after the acute respiratory illness. Donors 4 and 5 did not have any respiratory illness within the time frame of the collection of the 2 blood samples. Irradiated purified CD11b$^+$ cells were then added to allogenic PBLs and incubated with allogeneic irradiated DCs. Purified CD11b$^+$ cells were either untreated (black bars) or treated with either α-GalCer (100 ng/ml) in the presence of iNKT cells at a MDSC/iNKT ratio of 1:0.25 (white bars) or L-NMMA and NOHA (gray bars). The data are expressed as described in Methods. Addition of either iNKT cells or L-NMMA and NOHA to the alloreactive PBLs in the absence of CD11b$^+$ cells did not affect T cell proliferation (data not shown). The ratio of irradiated DCs to purified irradiated CD11b$^+$ cells was 1:1.

in the absence of detectable IAV-specific Ab response (Table 1). As a further control, we showed that CD11b$^+$ cells collected at different time points from individuals with undetectable IAV-specific Ab and without acute respiratory illness symptoms failed to inhibit MLR proliferation (Figure 7, D and E, and Table 1). The suppressive activity of MDSCs (i.e., CD11b$^+$ cells) collected from IAV-infected individuals could be reduced in vitro by incubating MDSCs with either ARG1 and NOS2 inhibitors or with α-GalCer in the presence of iNKT cells (Figure 7), at a MDSC/iNKT cell ratio (1:0.25) that did not cause iNKT cell–dependent MDSC lysis (Supplemental Figure 7B) and yet was capable of activating iNKT cells (Supplemental Figure 7C). Finally, we collected blood samples from 5 additional individuals within a short time (between 15 and 30 days) after onset of acute respiratory illness. Although for these donors, we did not have access to blood samples collected before the onset of the acute respiratory illness, we demonstrated the presence of high H3N2 (donors 6 and 10) and H1N1 (donors 7–9) IAV–specific Ab titer (Table 1) and demonstrated the suppressive activity of CD11b$^+$ cells, which was relieved by ARG1 and NOS2 inhibitors or by activating iNKT cells (Supplemental Figure 7A).

In conclusion, these results demonstrate the expansion of monocytes with a suppressive phenotype during acute IAV infections, which can be markedly reduced either by inhibiting the activity of ARG1 and NOS2 or harnessing iNKT cells.

Discussion

The results of the experiments described in this study highlight 3 main findings: (a) the enhanced susceptibility of *Jα18*$^{-/-}$ and *CD1d*$^{-/-}$ mice to PR8 infection; (b) the expansion of MDSCs with a suppressive phenotype during PR8 infection in *Jα18*$^{-/-}$ and *CD1d*$^{-/-}$ mice; and (c) the ability of adoptively transferred iNKT cells to markedly reduce the suppressive activity of MDSCs in *Jα18*$^{-/-}$ mice but not in *CD1d*$^{-/-}$ mice, hence restoring immunocompetence and ability to clear PR8 infection. Finally, we showed the presence of myeloid cells with a suppressive phenotype in PBMCs of IAV-infected individuals and the ability of human iNKT cells to abolish their suppressive phenotype. These results underscore what we believe to be a novel role of iNKT cells, as cells capable of modulating immunological suppressive mechanisms that are activated during acute inflammatory processes.

Although the mechanisms by which PR8 infection induces increased mortality of *Jα18*$^{-/-}$ and *CD1d*$^{-/-}$ mice and expansion of MDSCs remain unclear, chemokines (i.e., IP-10, MCP-1, and the neutrophil chemoattractant IL-8) and cytokines were shown to be elevated during IAV infection (3, 41). Recent results have shown that mice infected with the 1918 pandemic virus and highly pathogenic H5N1 virus elicit high levels of proinflammatory cytokines and lung infiltration of macrophages and neutrophils (55). These results were further extended in macaques with a lethal infection

of 1918 influenza virus (2) and were consistent with postmortem studies in patients infected with the human IAV H5N1, which demonstrated a predominance of macrophages and neutrophils in pulmonary infiltrates (3). Our studies support these findings, as the lungs of PR8-infected *Jα18*$^{-/-}$ and *CD1d*$^{-/-}$ mice are infiltrated by large numbers of a heterogeneous population of cells, endowed with the ability to suppress T cell proliferation and expressing markers of macrophages and neutrophils, as defined by the expression of CD11b, Gr-1, and 7/4 markers. Consistent with our observation that the suppressive activity of lung-infiltrating MDSCs can be relieved by using ARG1 and NOS2 inhibitors, it has previously been shown that neutrophils express both ARG1 and NOS2 and that these cells are capable of suppressing T cell proliferation by reducing arginine levels through ARG1 activity (56, 57).

It is likely that the effect of iNKT cells in controlling PR8 infection is mediated by several mechanisms, including their ability to assist T and B cell responses by maturing DCs and activating B cells (58–60). It is also known that secretion of IFN-γ and IL-12, resulting from activation of iNKT cells and DCs, selectively induces bystander activation of NK cells, B cells, and CD4$^+$ T cells and CD8$^+$ cytotoxic T lymphocytes (61–63). Consistent with this notion, it has been shown that activation of iNKT cells enhances NK-dependent murine cytomegalovirus (MCMV) immune response (64). Our results extend these previous findings by demonstrating that iNKT cells can restore the expansion of PR8-specific immune responses by relieving the suppression imposed by MDSCs and restoring PR8-specific immune responses. Although crosstalk between iNKT cells and CD11b$^+$Gr-1$^+$ cells has previously been described (65–67), these studies did not analyze the suppressive activity of CD11b$^+$Gr-1$^+$ cells on antigen-specific T cells.

The activation of iNKT cells by TLR-L–treated BM-derived MDSCs may be accounted for by many mechanisms, including enhanced secretion of soluble factors and increased expression of CD1d and costimulatory molecules (20, 47). Furthermore, incubation of BM-derived MDSCs with TLR-L may result in the upregulation of endogenous iNKT cell ligand(s), as TLR signaling events can modulate the lipid biosynthetic pathways of human and mouse DCs (45, 46). Although all these factors may contribute to the crosstalk between iNKT cells and TLR-L–treated BM-derived MDSCs, the lack of iNKT cell activation using either MDSCs from mice with GSL storage disease or MDSCs pretreated with the GSL inhibitor *N*B-DGJ indicate that conditions preventing optimal synthesis and/or loading of endogenous ligand(s) onto CD1d molecules may compromise the crosstalk between iNKT cells and MDSCs. Since it is known that IAV infection matures DCs mainly by binding of single-stranded RNA (ssRNA) to TLR7 (68) and of ssRNA bearing 5′-phosphates to retinoic acid–inducible gene I (RIG-I) (69, 70), it is possible that PR8-dependent activation of MDSCs could be due to similar mechanisms. We observed that LPS can facilitate the crosstalk between human MDSCs and iNKT cells. In contrast, the suppressive activity of mouse MDSCs is not reduced by the TLR4 agonist LPS or by its nontoxic derivative MPL, at a broad range of different concentrations, while the amount of IL-12p40 is significantly enhanced. The dichotomy of TLR4 signaling events in the suppressive activity of mouse and human MDSCs is of interest and warrants further investigation.

Since MDSCs have previously been described mainly in tumor models, it is important to compare the frequency and activity of MDSCs expanded during viral infections and tumor growth. While it was shown that the frequency of MDSCs in tumor-bearing WT mice continued to increase in proportion to tumor size (15), injection of sublethal doses of PR8 (300 PFU) showed that the highest frequency of lung-infiltrating MDSCs occurred during the acute phase of the infection and peaked at approximately day 20 after the infection. Similar kinetics of MDSC expansion was seen after injection of the less-aggressive H17 IAV (H3N2) (71) into *Jα18*$^{-/-}$ mice, which only caused severe weight loss in infected mice and a peak of lung-infiltrating MDSCs at day 9 after the infection (Supplemental Figure 6 and data not shown). Continuing expansion of the numbers of MDSCs during tumor growth and the ability of MDSCs purified from tumor-bearing, as compared with PR8-infected WT mice, to inhibit T cell proliferation could be accounted for by the hypothesis that the balance between MDSC activatory and inhibitory mechanisms is skewed in tumor-bearing mice toward immunosuppression and MDSC expansion. This may be due to tumor-dependent activation of type II NKT cells, previously shown to enhance MDSC suppressive activity (72), combined with the relatively low quantity of TLR-Ls. In contrast, the abundance of TLR-Ls during microbial infections, as compared with during tumor growth, activates iNKT cells, which provides more efficient control of the MDSC suppressive activity.

Finally, we extended the results obtained from IAV-infected mice to human-derived MDSCs. We showed that the suppressive effect of GM-CSF–treated CD11b$^+$ monocytes could be significantly reduced either by the addition of ARG1 and NOS inhibitors or by harnessing iNKT cell activity via TLR-L treatment or PR8 infection. More importantly, we showed that, unlike CD11b$^+$ monocytes from healthy donors, CD11b$^+$ monocytes collected within a short time after IAV infection and tested without incubation with GM-CSF were capable of suppressing MLR proliferation. Their treatment with either ARG1 and NOS inhibitors or with α-GalCer and iNKT cells restored normal T cell proliferation. A more in-depth analysis is warranted to establish the kinetics of MDSC expansion during IAV infection and to compare the frequency of MDSCs with both the numbers of iNKT cells and the activity of IAV-specific CD8$^+$ and CD4$^+$ T cells.

In conclusion, our results identify the interaction between iNKT cells and MDSCs as an important mechanism modulating MDSC suppressive activity during IAV infection. Since MDSCs also expand in cancer patients (9), our observation that iNKT cells play a central role in augmenting both T and B cell anti-IAV responses by abolishing MDSC suppressive activity suggests that harnessing iNKT cell activity should be considered as a treatment during viral infections and tumor growth.

Methods

Reagents. $UTY_{246–254}$ H-2D^b, $NP_{366–374}$ H-2D^b, and $OVA_{257–264}$ H-2K^b fluorescent tetrameric complexes (tetramers) (58) and CD1d/α-GalCer tetramers (73) were prepared as previously described. α-GalCer was solubilized at 200 μg/ml in vehicle (0.5% Tween-20/PBS). The Abs used for FACS analysis were CD11b, Gr-1–biotin/streptavidin, CD86, CD11c, MHC class II, and TLR9 (all from eBioscience); and CD1d, CD40, CD3, and CD8 (BD). Dead cells were stained with bisbenzimide (Sigma-Aldrich) or propidium iodide (Sigma-Aldrich). Samples were acquired on a FACSCalibur with CellQuest software (BD) or on a CyAn cytometer (Dako) and analyzed with FlowJo software. The anti–CD40 agonist Ab was provided by P. Lane (University of Birmingham) (74), and the anti–mouse CD1d blocking Ab 3C11 was provided by J. Yewdell (NIH, Bethesda, Maryland, USA). Influenza virus strain PR8 (H1N1) was provided by Keith Gould (Imperial College London, London, United Kingdom) (38). Vaccinia virus encoding the $UTY_{246–254}$

was engineered and expanded as previously described (75). NOS2 and ARG1 inhibitors N^G-monomethyl-L-arginine (L-NMMA; Calbiochem) and *N*-hydroxy-L-arginine (NOHA; Calbiochem) were used at 500 μM and added to cultures containing MDSCs, DCs, and T lymphocytes.

Mice. All mice were maintained in the Biological Services Unit, John Radcliffe Hospital, University of Oxford. Approval of care and use was obtained from the Clinical Medicine Ethical Review Committee, University of Oxford, under the authority of a UK home office project license. Female C57BL/6 (B6) mice (aged 6–8 weeks) were used. *CD1d*$^{-/-}$ mice were provided by L. Van Kaer (Vanderbilt University School of Medicine, Nashville, Tennessee, USA) (76) and were backcrossed 10 times onto the B6 background. Also used were mice lacking the *Jα18* TCR gene segment (77), which were devoid of Vα14 iNKT cells, while having other lymphoid cell lineages intact (iNKT$^{-/-}$ mice). *CD40L*$^{-/-}$ and *CD40*$^{-/-}$ mice were purchased from The Jackson Laboratory and backcrossed 10 times onto the B6 background (78). The *Hex*β$^{-/-}$ (79) and *iGb3S*$^{-/-}$ (53) mice were maintained and genotyped according to published methods. Sandhoff *Hex*β$^{-/-}$ (mouse model of Sandhoff disease) and *iGb3S*$^{-/-}$ mice had been backcrossed at least 6 times before use. Heterozygote littermates and age-matched B6 mice, as appropriate, were used as controls. OT-I TCR transgenic mice were provided by M. Merckenschlager (Imperial College London) and backcrossed 8 times onto the B6 background.

In vivo PR8 infection. Female B6 mice (aged 6–8 weeks) were inoculated intranasally with 3×10^4 PFU of PR8.

Virus titer. To quantify PR8 virus titer, lungs from PR8-infected mice were harvested 3 days after infection and homogenized. Confluent monolayers of MDCK cells were incubated with 3-fold dilutions of lung homogenates at 37°C for 30 minutes. Equal volumes of type I agarose (1.8% in distilled water, and autoclaved) (Sigma-Aldrich) and MEM containing 2% BSA, 1% glutamine, and 1 μg/ml trypsin (Sigma-Aldrich) were heated at 42°C for at least 45 minutes before mixing and overlaying on infected cells. Agarose layers were left to set at room temperature. The plates were incubated at 37°C and plaques counted on day 2. The MDCK cell monolayers were fixed and stained with fixing solution (37% formaldehyde and 1% crystal violet) overnight. The plates were then washed and plaques were counted. PFU per lung was determined according to the equation PFU = number of plaques × dilution factor × (total volume of lung homogenate/volume of dilution added to monolayers).

Isolation and culture of mouse MDSCs. For purification of MDSCs from PR8-infected mice, lungs were collected within 4–6 days after infection of mice with PR8 (3×10^4 PFU/mouse) and digested with collagenase type 2 (Worthington Biochemical Corp.) for 20 minutes. MDSCs were purified from lung homogenates using biotin-conjugated rat anti–mouse Gr-1 Ab and streptavidin-coated magnetic beads following the manufacturer's instructions (Miltenyi Biotec). For purification of mouse BM-derived MDSCs, BM cells were cultured in complete medium with 1 ng/ml GM-CSF. On day 5, CD11c$^+$ cells were removed with anti-CD11c–coated magnetic beads (Miltenyi Biotec), and Gr-1$^+$CD11b$^+$CD11c$^-$ cells were purified using biotin-conjugated rat anti–mouse Gr-1 Abs (eBioscience) and streptavidin-coated magnetic beads (Miltenyi Biotec). BM-derived MDSCs (1×10^6/well) were treated with (a) α-GalCer (0.4 μg/ml); (b) TLR-Ls poly I:C (0.4 μg/ml; Sigma-Aldrich), R848 (0.4 μg/ml; PharmaTech), or CpG 2216 (4 μg/ml; GGGGGACGATCGTCGGGGGG; Coley, Pfizer) in complete medium for 48 hours; or (c) PR8 (2.5×10^4 PFU) in RPMI at 37°C, 5% CO_2 for 1 hour, washed 3 times, and cocultured with liver-purified iNKT cells or OT-I splenocytes.

Identification of human subjects. Samples from 89 healthy volunteers were collected over a 24-month period. Sampling involved taking whole blood PBMCs, with residual sera/plasma collected and retained for Ab assays. Informed consent was obtained from all participating individuals prior to the study. Ethical approval was obtained from the Oxford Tropical Research Ethics Committee (OXTREC), University of Oxford.

Isolation and differentiation of human MDSCs. Human MDSCs were generated from peripheral blood monocytes. Healthy donor MDSCs were differentiated from CD11b$^+$ cells by culturing them with 5 ng/ml GM-CSF for 4 days, using a recently described protocol (54). MDSCs purified from IAV-infected patients were sorted from PBMCs using CD11b beads. α-GalCer and TLR-L were added to human MDSCs for 24 hours in the presence of iNKT cells. PR8 (2.5×10^4 PFU) was added to MDSCs in RPMI at 37°C, 5% CO_2 for 1 hour, and then cells were washed 3 times and cocultured with iNKT cells for 24 hours and then irradiated (50 Gy).

Isolation of mouse iNKT cells. Liver iNKT cells were prepared by generating single-cell suspensions of perfused livers of naive WT mice. iNKT cells were enriched by overlaying 80% Percoll with cells resuspended in 40% Percoll. Cells were centrifuged at room temperature at 1,783 *g* continuously for 25 minutes. Cells were collected from the interphase, and iNKT cells were further enriched by sorting with anti–TCR-β and anti-CD5 Abs (eBioscience). In all the experiments shown, the percentage of iNKT cells, as measured by CD1d/α-GalCer tetramer staining, was greater than 50%. This protocol was very reproducible, as iNKT cell frequency was less than 50% in only 1 experiment, where it was 14% (data not shown). Sorting with anti–TCR-β Ab did not activate iNKT cells, as shown by the lack of IFN-γ and IL-4 secretion by sorted iNKT cells (see Figures 4 and 5). In the experiment shown in Supplemental Figure 1, liver-purified iNKT cells were simultaneously stained with anti-CD5 and anti–TCR-β Abs and CD1d/α-GalCer tetramers, and triple-positive cells, representing 75% of the total population, were removed. In the adoptive transfer experiments, 3×10^5 iNKT cells were transferred i.v. into PR8-infected mice, 24 hours after the infection. iNKT cells were purified following the protocol described above from either WT mice or from *Vα14* TCR transgenic mice (80), provided by A. Lehuen (INSERM U561, Hôpital Saint Vincent de Paul, Paris, France), using only Percoll gradient purification, without sorting with anti–TCR-β and anti-CD5 Abs.

Human iNKT cells. iNKT cells were generated from healthy blood donors as described by Salio et al. (45).

Mouse DC differentiation. Mouse DCs were differentiated from BM in complete medium in the presence of 20 ng/ml GM-CSF and 20 ng/ml IL-4 (Peprotech) for 7 days. Fresh complete medium, GM-CSF, and IL-4 were added every 2 days.

Human DCs. Human DCs were generated by culturing monocytes for 4 days in RPMI/10% FCS supplemented with 50 ng/ml GM-CSF (Peprotech) and 1,000 U/ml IL-4 (45).

OT-I proliferation assays. Splenocytes from OT-I TCR transgenic mice were pulsed with 2 μg/ml of SIINFEKL peptide for 1 hour at 37°C, washed, and labeled with 5 μM CFSE. Treated or untreated MDSCs (3×10^4) were cultured in 96-well flat-bottom plates with 3×10^5 CFSE-labeled OT-I splenocytes. Cells were analyzed using a FACSCalibur with CellQuest software 4 days later. The data are expressed as the percentage of proliferation of SIINFEKL peptide–pulsed and CFSE-labeled-OT-I splenocytes in the presence of MDSCs compared with proliferation of SIINFEKL peptide–pulsed and CFSE-labeled OT-I splenocytes in the absence of MDSCs (100%). The addition of L-NMMA and NOHA to OT-I splenocytes in the absence of MDSCs did not affect OT-I proliferation (data not shown).

Measuring activity of MDSC enzymes. ARG1 and NOS2 activities of α-GalCer–pulsed BM-derived MDSCs cocultured with BM-derived iNKT cells were assessed at different time points. NOS2 activity was measured from supernatants by Griess reaction as the amount of NO_3^- and NO_2^- produced using a nitrate/nitrite assay kit (Cayman Chemical) (17). ARG1 activity was measured in cell lysates, as previously described (17).

Prime-boost vaccination. MDSCs (5×10^6) purified from female mice were injected i.v. into female recipients. On the same day, BM-derived DCs (1×10^6) from male mice, were injected i.v. in the opposite tail vein. A week later,

mice were boosted with 10^6 PFU of UV-inactivated vaccinia virus encoding the $UTY_{246–254}$ peptide (75).

Anti-IAV Ab measurements. Plasma taken from 89 individuals was stored at –80°C prior to assay for the presence of HI Abs. Samples were treated with receptor-destroying enzyme for 16 hours at 37°C (13 v/v), followed by inactivation at 56°C (RDE; Denka Seiken Co.). HI assays were performed in duplicate using standard protocols (81), with whole virus antigens representing IAVs circulating during the winter seasons of 2006–2007 and 2007–2008. Influenza virus A/Solomon Islands/3/2006 and A/New Caledonia/20/99 (H1N1 strains) and A/Wisconsin/67/2005 and A/Wellington/1/2004 (H3N2 strains) circulated during the time period over which the human blood samples were collected. The HI Ab titer was calculated as the highest dilution that completely prevented agglutination. The final titer was the geometric mean of the duplicates. Sequential sera from the same individual were assayed simultaneously. Four-fold or greater rises in HI Ab titer between preinfection and post-illness sera were considered indicative of recent infection.

MLR. PBLs (2×10^5) were mixed with allogeneic irradiated (50 Gy) DCs (5×10^4) in 200 μl of RPMI 5% human AB serum in 96-well flat-bottom plates. Cells were incubated at 37°C, 5% CO_2 for 5 days, and then 1 μCi/well [^{3}H]thymidine (PerkinElmer) was added for 15–18 hours. [^{3}H]thymidine incorporation was measured using a Wallac MicroBeta JET 1450 reader (PerkinElmer). MDSC-mediated inhibition of lymphocyte proliferation was carried out by coculturing irradiated MDSCs (5×10^4), from either healthy donors or influenza virus–infected patients, together with PBLs and irradiated DCs. The data are expressed as the percentage of PBL proliferation driven by allogeneic irradiated DCs in the presence of irradiated MDSCs compared with alloreactive PBL proliferation in the absence of MDSCs (100%).

ELISA. For measurement of cytokine production, supernatants of MDSCs cocultured with BM-derived iNKT cells were collected at different time points. The amount of IL-12p40, IFN-γ, and IL-4 was measured using an ELISA kit (eBioscience). For measurement of IgG Ab levels, sera from PR8-infected mice were collected 6 days after infection and Ab titers were determined by coating 96-well NUNC MaxiSorp plates with 5 μg/ml of PR8 virus overnight at 4°C. The plates were washed with PBS and blocked with 1% of BSA for 1 hour at room temperature. Serial dilutions of the serum samples were plated for 2 hours at room temperature. Plates were then washed, and HRP-coupled goat anti–mouse IgG was added for 1 hour. Color reactions were developed with 3,3′,5-5′-tetramethylbenzidine (TMB; Sigma-Aldrich), and the absorbance was measured at 490 nm.

RT-PCR. Human and mouse MDSCs that were infected in vitro or in vivo were checked for infection by RT-PCR using the following NP primers: forward, TGATCGGAACTTCTGGAGGG and reverse, TGGCCCAGTACCTGCTTCTC. As control, we used mouse GAPDH — forward, CCAGGTTGTCTGCGACTT and reverse, CCTGTTGCTGTAGCCGTATTC; human GAPDH-reverse primer — forward, CCAGCCGAGCCACATCGCTC and reverse, ATGAGCCCCAGCCTTCTCCAT.

Statistics. Two-tailed Student's *t* test was used to compare the significance of the difference between the mean of 2 groups in relation to the variation in the data. *P* values of 0.05 or less were considered significant. Error bars in all figures denote SD.

Acknowledgments

This work was funded by Cancer Research UK grant C399/A2291 (to C. De Santo, M. Salio, S.H. Masri, and V. Cerundolo), the UK Medical Research Council (to V. Cerundolo), and Deutsche Forschungsgemeinschaft grant SFB 405:B10 (to H.-J. Gröne). F.M. Platt is supported by the University of Oxford Department of Pharmacology. G.S. Besra acknowledges support in the form of a Personal Research Chair from James Bardick, as a former Lister Institute-Jenner Research Fellow, grants from the MRC and the Wellcome Trust, and the Royal Society Wolfson Research Merit Award. A.O. Speak is funded by the MRC. We thank Alain Townsend, Andrew McMichael, Angus Stock, and Jonathan Silk for critical reading of the manuscript and Paolo Polzella and Dipa Lackmann for technical support.

Received for publication May 21, 2008, and accepted in revised form October 15, 2008.

Address correspondence to: Vincenzo Cerundolo, MRC Human Immunology Unit, Weatherall Institute of Molecular Medicine, John Radcliffe Hospital, Oxford OX3 9DS, United Kingdom. Phone: 44-1865-222412; Fax: 44-1865-222502; E-mail: vincenzo.cerundolo@imm.ox.ac.uk.

1. Palese, P. 2004. Influenza: old and new threats. *Nat. Med.* **10**:S82–S87.
2. Kobasa, D., et al. 2007. Aberrant innate immune response in lethal infection of macaques with the 1918 influenza virus. *Nature.* **445**:319–323.
3. de Jong, M.D., et al. 2006. Fatal outcome of human influenza A (H5N1) is associated with high viral load and hypercytokinemia. *Nat. Med.* **12**:1203–1207.
4. Doherty, P.C., et al. 1997. Effector CD4+ and CD8+ T-cell mechanisms in the control of respiratory virus infections. *Immunol. Rev.* **159**:105–117.
5. Delano, M.J., et al. 2007. MyD88-dependent expansion of an immature GR-1+CD11b+ population induces T cell suppression and Th2 polarization in sepsis. *J. Exp. Med.* **204**:1463–1474.
6. Mencacci, A., et al. 2002. CD80+Gr-1+ myeloid cells inhibit development of antifungal Th1 immunity in mice with candidiasis. *J. Immunol.* **169**:3180–3190.
7. Bronte, V., et al. 2000. Identification of a CD11b(+)/Gr-1(+)/CD31(+) myeloid progenitor capable of activating or suppressing CD8(+) T cells. *Blood.* **96**:3838–3846.
8. Almand, B., et al. 2001. Increased production of immature myeloid cells in cancer patients: a mechanism of immunosuppression in cancer. *J. Immunol.* **166**:678–689.
9. Ochoa, A., Zea, A., Hermandez, C., and Rodriguez, P.C. 2007. Arginase, prostaglandins, and myeloid derived suppressor cells in renal cell carcinoma. *Clin. Cancer Res.* **13**:721s–726s.
10. Bronte, V., and Zanovello, P. 2005. Regulation of immune responses by L-arginine metabolism. *Nat. Rev. Immunol.* **5**:641–654.
11. Yu, H., Kortylewski, M., and Pardoll, D. 2007. Crosstalk between cancer and immune cells: role of STAT3 in the tumour microenvironment. *Nat. Rev. Immunol.* **7**:41–51.
12. Gabrilovich, D.I., et al. 2007. The terminology issue for myeloid-derived suppressor cells. *Cancer Res.* **67**:425; author reply 426.
13. Kusmartsev, S., and Gabrilovich, D.I. 2005. STAT1 signaling regulates tumor-associated macrophage-mediated T cell deletion. *J. Immunol.* **174**:4880–4891.
14. Lin, H., et al. 2005. The macrophage F4/80 receptor is required for the induction of antigen-specific eferent regulatory T cells in peripheral tolerance. *J. Exp. Med.* **201**:1615–1625.
15. Gallina, G., et al. 2006. Tumors induce a subset of inflammatory monocytes with immunosuppressive activity on CD8+ T cells. *J. Clin. Invest.* **116**:2777–2790.
16. Bronte, V., et al. 2003. IL-4-induced arginase 1 suppresses alloreactive T cells in tumor-bearing mice. *J. Immunol.* **170**:270–278.
17. De Santo, C., et al. 2005. Nitroaspirin corrects immune dysfunction in tumor-bearing hosts and promotes tumor eradication by cancer vaccination. *Proc. Natl. Acad. Sci. U. S. A.* **102**:4185–4190.
18. Serafini, P., et al. 2006. Phosphodiesterase-5 inhibition augments endogenous antitumor immunity by reducing myeloid-derived suppressor cell function. *J. Exp. Med.* **203**:2691–2702.
19. Terabe, M., et al. 2006. CD1d-restricted natural killer T cells can down-regulate tumor immunosurveillance independent of interleukin-4 receptor-signal transducer and activator of transcription 6 or transforming growth factor-beta. *Cancer Res.* **66**:3869–3875.
20. Brigl, M., Bry, L., Kent, S.C., Gumperz, J.E., and Brenner, M.B. 2003. Mechanism of CD1d-restricted natural killer T cell activation during microbial infection. *Nat. Immunol.* **4**:1230–1237.
21. Crowe, N.Y., et al. 2005. Differential antitumor immunity mediated by NKT cell subsets in vivo. *J. Exp. Med.* **202**:1279–1288.
22. Mattner, J., et al. 2005. Exogenous and endogenous glycolipid antigens activate NKT cells during microbial infections. *Nature.* **434**:525–529.
23. Kinjo, Y., et al. 2005. Recognition of bacterial glycosphingolipids by natural killer T cells. *Nature.* **434**:520–525.
24. Kawakami, K., et al. 2001. Monocyte chemoattractant protein-1-dependent increase of V alpha 14 NKT cells in lungs and their roles in Th1 response and host defense in cryptococcal infection. *J. Immunol.* **167**:6525–6532.

25. Duthie, M.S., et al. 2002. During Trypanosoma cruzi infection CD1d-restricted NK T cells limit parasitemia and augment the antibody response to a glycophosphoinositol-modified surface protein. *Infect. Immun.* **70**:36–48.
26. Amprey, J.L., Spath, G.F., and Porcelli, S.A. 2004. Inhibition of CD1 expression in human dendritic cells during intracellular infection with Leishmania donovani. *Infect. Immun.* **72**:589–592.
27. Grubor-Bauk, B., Simmons, A., Mayrhofer, G., and Speck, P.G. 2003. Impaired clearance of herpes simplex virus type 1 from mice lacking CD1d or NKT cells expressing the semivariant V alpha 14-J alpha 281 TCR. *J. Immunol.* **170**:1430–1434.
28. Ashkar, A.A., and Rosenthal, K.L. 2003. Interleukin-15 and natural killer and NKT cells play a critical role in innate protection against genital herpes simplex virus type 2 infection. *J. Virol.* **77**:10168–10171.
29. Broxmeyer, H.E., et al. 2007. A role for natural killer T cells and CD1d molecules in counteracting suppression of hematopoiesis in mice induced by infection with murine cytomegalovirus. *Exp. Hematol.* **35**:87–93.
30. Kakimi, K., Guidotti, L.G., Koezuka, Y., and Chisari, F.V. 2000. Natural killer T cell activation inhibits hepatitis B virus replication in vivo. *J. Exp. Med.* **192**:921–930.
31. Exley, M.A., et al. 2001. CD1d-reactive T-cell activation leads to amelioration of disease caused by diabetogenic encephalomyocarditis virus. *J. Leukoc. Biol.* **69**:713–718.
32. Johnson, T.R., Hong, S., Van Kaer, L., Koezuka, Y., and Graham, B.S. 2002. NK T cells contribute to expansion of CD8(+) T cells and amplification of antiviral immune responses to respiratory syncytial virus. *J. Virol.* **76**:4294–4303.
33. Yuan, W., Dasgupta, A., and Cresswell, P. 2006. Herpes simplex virus evades natural killer T cell recognition by suppressing CD1d recycling. *Nat Immunol* **7**:835–842.
34. Webb, T.J., et al. 2006. Inhibition of CD1d1-mediated antigen presentation by the vaccinia virus B1R and H5R molecules. *Eur. J. Immunol.* **36**:2595–2600.
35. Hage, C.A., et al. 2005. Human immunodeficiency virus gp120 downregulates CD1d cell surface expression. *Immunol. Lett.* **98**:131–135.
36. Ho, L.P., et al. 2008. Activation of invariant NKT cells enhances the innate immune response and improves the disease course in influenza A virus infection. *Eur. J. Immunol.* **38**:1913–1922.
37. Benton, K.A., et al. 2001. Heterosubtypic immunity to influenza A virus in mice lacking IgA, all Ig, NKT cells, or gamma delta T cells. *J. Immunol.* **166**:7437–7445.
38. Lubeck, M.D., Palese, P., and Schulman, J.L. 1979. Non random association of parental genes in inflenza A virus recombinants. *Virology.* **95**:269–273.
39. Pauksens, K., Fjaertoft, G., Douhan-Hakansson, L., and Venge, P. 2007. Neutrophil and monocyte receptor expression in uncomplicated and complicated influenza A infection with pneumonia. *Scand. J. Infect. Dis.* **40**:326–337.
40. Neff-LaFord, H., Teske, S., Bushnell, T.P., and Lawrence, B.P. 2007. Aryl hydrocarbon receptor activation during influenza virus infection unveils a novel pathway of IFN-gamma production by phagocytic cells. *J. Immunol.* **179**:247–255.
41. Cheung, C.Y., et al. 2002. Induction of proinflammatory cytokines in human macrophages by influenza A (H5N1) viruses: a mechanism for the unusual severity of human disease? *Lancet.* **360**:1831–1837.
42. Kusmartsev, S., Nagaraj, S., and Gabrilovich, D.I. 2005. Tumor-associated CD8+ T cell tolerance induced by bone marrow-derived immature myeloid cells. *J. Immunol.* **175**:4583–4592.
43. Ling, P., et al. 1995. Human IL-12 p40 homodimer binds to the IL-12 receptor but does not mediate biologic activity. *J. Immunol.* **154**:116–127.
44. Shimozato, O., et al. 2006. The secreted form of the p40 subunit of interleukin (IL)-12 inhibits IL-23 functions and abrogates IL-23-mediated antitumour effects. *Immunology.* **117**:22–28.
45. Salio, M., et al. 2007. Modulation of human natural killer T cell ligands on TLR-mediated antigen-presenting cell activation. *Proc. Natl. Acad. Sci. U. S. A.* **104**:20490–20495.
46. Paget, C., et al. 2007. Activation of invariant NKT cells by toll-like receptor 9-stimulated dendritic cells requires type I interferon and charged glycosphingolipids. *Immunity.* **27**:597–609.
47. Nagarajan, N.A., and Kronenberg, M. 2007. Invariant NKT cells amplify the innate immune response to lipopolysaccharide. *J. Immunol.* **178**:2706–2713.
48. Zhou, D., et al. 2004. Lysosomal glycosphingolipid recognition by NKT cells. *Science.* **306**:1786–1789.
49. Gadola, S.D., et al. 2006. Impaired selection of invariant natural killer T cells in diverse mouse models of glycosphingolipid lysosomal storage diseases. *J. Exp. Med.* **203**:2293–2303.
50. Schümann, J., et al. 2007. Differential alteration of lipid antigen presentation to NKT cells due to imbalances in lipid metabolism. *Eur J. Immunol.* **37**:1431–1441.
51. Platt, F.M., Neises, G.R., Dwek, R.A., and Butters, T.D. 1994. N-butyldeoxynojirimycin is a novel inhibitor of glycolipid biosynthesis. *J. Biol. Chem.* **269**:8362–8365.
52. Speak, A.O., et al. 2007. From the cover: implications for invariant natural killer T cell ligands due to the restricted presence of isoglobotrihexosylceramide in mammals. *Proc. Natl. Acad. Sci. U. S. A.* **104**:5971–5976.
53. Porubsky, S., et al. 2007. From the cover: normal development and function of invariant natural killer T cells in mice with isoglobotrihexosylceramide (iGb3) deficiency. *Proc. Natl. Acad. Sci. U. S. A.* **104**:5977–5982.
54. Chitta, S., Santambrogio, L., and Stern, L.J. 2008. GMCSF in the absence of other cytokines sustains human dendritic cell precursors with T cell regulatory activity and capacity to differentiate into functional dendritic cells. *Immunol. Lett.* **116**:41–54.
55. Perrone, L.A., Plowden, J.K., Garcia-Sastre, A., Katz, J.M., and Tumpey, T.M. 2008. H5N1 and 1918 pandemic influenza virus infection results in early and excessive infiltration of macrophages and neutrophils in the lungs of mice. *PLoS Pathog.* **4**:e1000115.
56. Jacobsen, L.C., Theilgaard-Monch, K., Christensen, E.I., and Borregaard, N. 2007. Arginase 1 is expressed in myelocytes/metamyelocytes and localized in gelatinase granules of human neutrophils. *Blood.* **109**:3084–3087.
57. Munder, M., et al. 2006. Suppression of T-cell functions by human granulocyte arginase. *Blood.* **108**:1627–1634.
58. Hermans, I.F., et al. 2003. NKT cells enhance CD4+ and CD8+ T cell responses to soluble antigen in vivo through direct interaction with dendritic cells. *J. Immunol.* **171**:5140–5147.
59. Fujii, S., Shimizu, K., Smith, C., Bonifaz, L., and Steinman, R.M. 2003. Activation of natural killer T cells by alpha-galactosylceramide rapidly induces the full maturation of dendritic cells in vivo and thereby acts as an adjuvant for combined CD4 and CD8 T cell immunity to a coadministered protein. *J. Exp. Med.* **198**:267–279.
60. Galli, G., et al. 2007. Invariant NKT cells sustain specific B cell responses and memory. *Proc. Natl. Acad. Sci. U. S. A.* **104**:3984–3989.
61. Eberl, G., Brawand, P., and MacDonald, H.R. 2000. Selective bystander proliferation of memory CD4+ and CD8+ T cells upon NK T or T cell activation. *J. Immunol.* **165**:4305–4311.
62. Eberl, G., and MacDonald, H.R. 2000. Selective induction of NK cell proliferation and cytotoxicity by activated NKT cells. *Eur. J. Immunol.* **30**:985–992.
63. Silk, J.D., et al. 2004. Utilizing the adjuvant properties of CD1d-dependent NK T cells in T cell-mediated immunotherapy. *J. Clin. Invest.* **114**:1800–1811.
64. van Dommelen, S.L., Tabarias, H.A., Smyth, M.J., and Degli-Esposti, M.A. 2003. Activation of natural killer (NK) T cells during murine cytomegalovirus infection enhances the antiviral response mediated by NK cells. *J. Virol.* **77**:1877–1884.
65. Li, L., et al. 2007. NKT cell activation mediates neutrophil IFN-gamma production and renal ischemia-reperfusion injury. *J. Immunol.* **178**:5899–5911.
66. Hwang, S.J., Kim, S., Park, W.S., and Chung, D.H. 2006. IL-4 secreting NKT cells prevent hypersensitivity pneumonitis by suppressing IFN-gamma producing neutrophils. *J. Immunol.* **177**:5258–5268.
67. Yanagisawa, K., et al. 2006. Hyporesponsiveness to natural killer T-cell ligand alpha-galactosylceramide in cancer-bearing state mediated by CD11b+ Gr-1+ cells producing nitric oxide. *Cancer Res.* **66**:11441–11446.
68. Pichlmair, A., and Reis e Sousa, C. 2007. Innate recognition of viruses. *Immunity.* **27**:370–383.
69. Pichlmair, A., et al. 2006. RIG-I-mediated antiviral responses to single-stranded RNA bearing 5′-phosphates. *Science.* **314**:997–1001.
70. Kato, H., et al. 2006. Differential roles of MDA5 and RIG-I helicases in the recognition of RNA viruses. *Nature.* **441**:101–105.
71. Townsend, A.R., and Skehel, J.J. 1984. The influenza A virus nucleoprotein gene controls the induction of both subtype specific and cross-reactive cytotoxic T cells. *J. Exp. Med.* **160**:552–563.
72. Terabe, M., et al. 2005. A nonclassical non-Valpha-14Jalpha18 CD1d-restricted (type II) NKT cell is sufficient for down-regulation of tumor immunosurveillance. *J. Exp. Med.* **202**:1627–1633.
73. Karadimitris, A., et al. 2001. Human CD1d-glycolipid tetramers generated by in vitro oxidative refolding chromatography. *Proc. Natl. Acad. Sci. U. S. A.* **98**:3294–3298.
74. Rolink, A., Melchers, F., and Andersson, J. 1996. The SCID but not the RAG-2 gene product is required for S mu-S epsilon heavy chain class switching. *Immunity.* **5**:319–330.
75. Palmowski, M.J., et al. 2006. Role of immunoproteasomes in cross-presentation. *J. Immunol.* **177**:983–990.
76. Mendiratta, S.K., et al. 1997. CD1d1 mutant mice are deficient in natural T cells that promptly produce IL-4. *Immunity.* **6**:469–477.
77. Cui, J., et al. 1997. Requirement for Valpha14 NKT cells in IL-12-mediated rejection of tumors. *Science.* **278**:1623–1626.
78. Li, Y., et al. 2007. B cells and T cells are critical for the preservation of bone homeostasis and attainment of peak bone mass in vivo. *Blood.* **109**:3839–3848.
79. Sango, K., et al. 1996. Mice lacking both subunits of lysosomal beta-hexosaminidase display gangliosidosis and mucopolysaccharidosis. *Nat. Genet.* **14**:348–352.
80. Laloux, V., Beaudoin, L., Ronet, C., and Lehuen, A. 2002. Phenotypic and functional differences between NKT cells colonizing splanchnic and peripheral lymph nodes. *J. Immunol.* **168**:3251–3258.
81. Zambon, M. 1998. Laboratory diagnosis of influenza. In *Textbook of influenza.* R.G. Webster, A.J. Hay, and K. Nicolson, editors. Blackwell Science. London, United Kingdom. 291–313.